YMTHE, Volume *28*

Supplemental Information

Imaging CAR T Cell Trafficking with eDHFR as a PET Reporter Gene

Mark A. Sellmyer, Sarah A. Richman, Katheryn Lohith, Catherine Hou, Chi-Chang Weng, Robert H. Mach, Roddy S. O'Connor, Michael C. Milone, and Michael D. Farwell

Imaging CAR T Cell Trafficking with eDHFR as a PET Reporter Gene

Mark A. Sellmyer[1,2†*], Sarah A. Richman[3†], Katheryn Lohith[1], Catherine Hou[1], Chi-Chang Weng[1,4], Robert H. Mach[1], Roddy S. O'Connor[5], Michael C. Milone[5], and Michael D. Farwell[1*]

[1]Department of Radiology, University of Pennsylvania, Philadelphia, PA 19104, USA;

[2]Department of Biochemistry and Biophysics, University of Pennsylvania;

[3]Division of Oncology, Department of Pediatrics, Children's Hospital of Philadelphia and Perelman School of Medicine at the University of Pennsylvania;

[4]Department of Medical Imaging and Radiological Sciences, Chang Gung University, Taoyuan, Taiwan;

[5]Department of Pathology and Laboratory Medicine, University of Pennsylvania.

Short Title: CAR T cell PET reporter gene imaging

Keywords: CAR T Cells, reporter gene, molecular imaging

† Co-first authorship

* Correspondence should be addressed to:

M.D.F. (michael.farwell@pennmedicine.upenn.edu) or

M.A.S. (mark.sellmyer@pennmedicine.upenn.edu)

https://orcid.org/0000-0002-1407-1905

Department of Radiology

Perelman School of Medicine at the University of Pennsylvania

813A Stellar-Chance Labs

422 Curie Boulevard

Philadelphia, PA

19104-6059

Phone: 215-573-3212

	eDHFR 116		**10 μM MTX**		**10 μM TMP**	
	Mean	**SD**	**Mean**	**SD**	**Mean**	**SD**
5 min	14.3	1.87	17.2	1.03	5.82	1.1
30 min	47.2	1.84	30.4	1.29	6.66	0.48
60 min	87.1	4.82	18.8	1.84	7.04	0.7
120 min	134.6	2.71	9.42	0.73	8.38	1.13

	Control 116		**10 μM MTX**		**10 μM TMP**	
	Mean	**SD**	**Mean**	**SD**	**Mean**	**SD**
5 min	5.11	0.49	6.32	0.41	5.37	0.78
30 min	6.58	0.51	5.59	0.43	5.83	0.48
60 min	7.37	0.62	6.74	0.63	6.48	0.52
120 min	8.4	0.52	8.62	0.66	7.61	0.33

Figure S1. Tabular evaluation of eDHFR and Control 116 [^{18}F]-TMP uptake with competitive inhibitors. Values displayed are in % Input / 100 μg Protein (n=4).

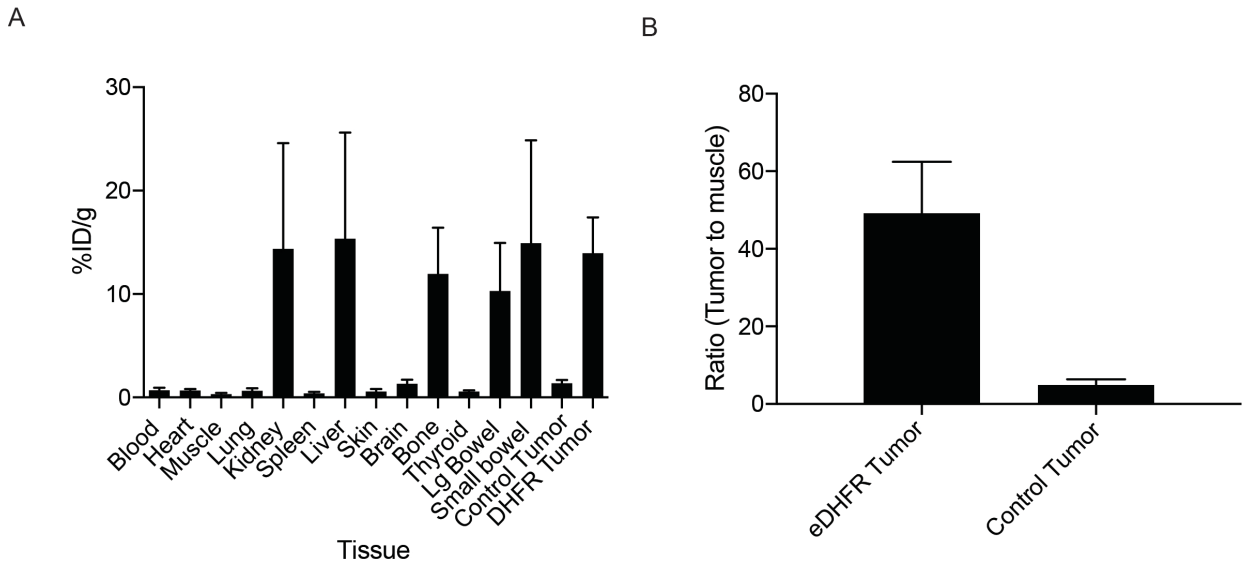

Figure S2. Ex vivo biodistribution of tissues including eDHFR and control HCT116 tumors. Mice were sacrificed at the completion of the PET/CT imaging session. **A)** Uptake in percent injected dose per gram (%ID/g) was assayed with a gamma counter (n=3). **B)** Ratio of tumor uptake to muscle (n=3). Error bars represent the standard deviation.

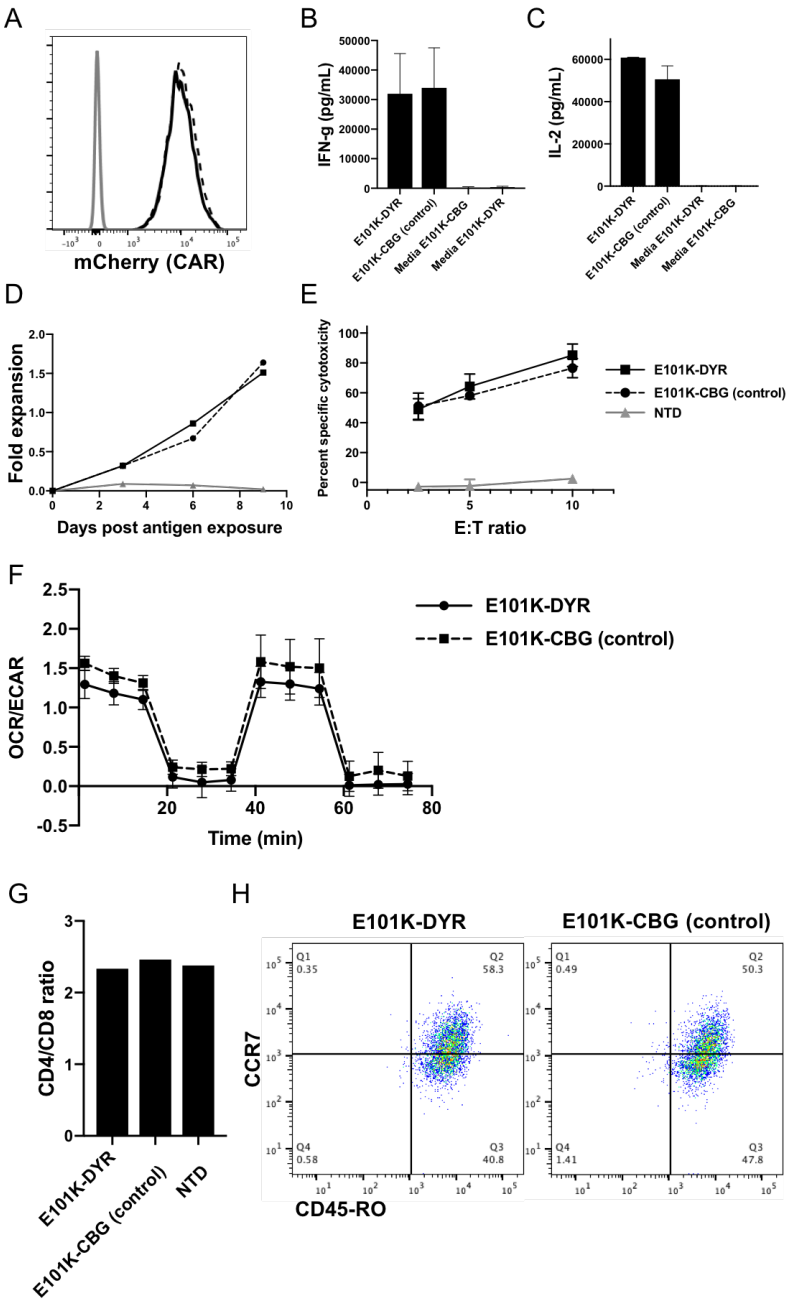

Figure S3. In vitro effector function, metabolic profile, and subset profile of CAR-DYR T cells. Sorted primary human T cells co-expressing the GD2-E101K CAR-T2A-mCherry and either DYR (E101K-DYR) or control construct consisting of GFP and click beetle green luciferase (E101K-CBG) were used in the following assays A) Flow cytometry comparing mCherry (CAR) expression of sorted cells prior to antigen exposure. Following exposure to GD2^{+} SY5Y target cells, IL-2 and IFN-γ secretion was determined by ELISA (B-C). Fold population expansion was determined by flow cytometric bead-based counting (D). Cytotoxicity was determined by ^{51}Cr release assay (E). Oxygen consumption rate (OCR) and extracellular acidification rate (ECAR) were

determined via Seahorse assay (F). The ratio of $CD4^+$ and $CD8^+$ T cells, as well as the proportion of $CD45\text{-}RO^+/CCR7^+$ cells (central memory) was determined by flow cytometry. Data are from one T cell donor. Graphs show mean with error bars showing SD. Cytokine release and cytotoxicity assays were performed in triplicate. Seahorse assay was performed with 14 replicates for E101K-DYR and 10 replicates for E101K-CBG.

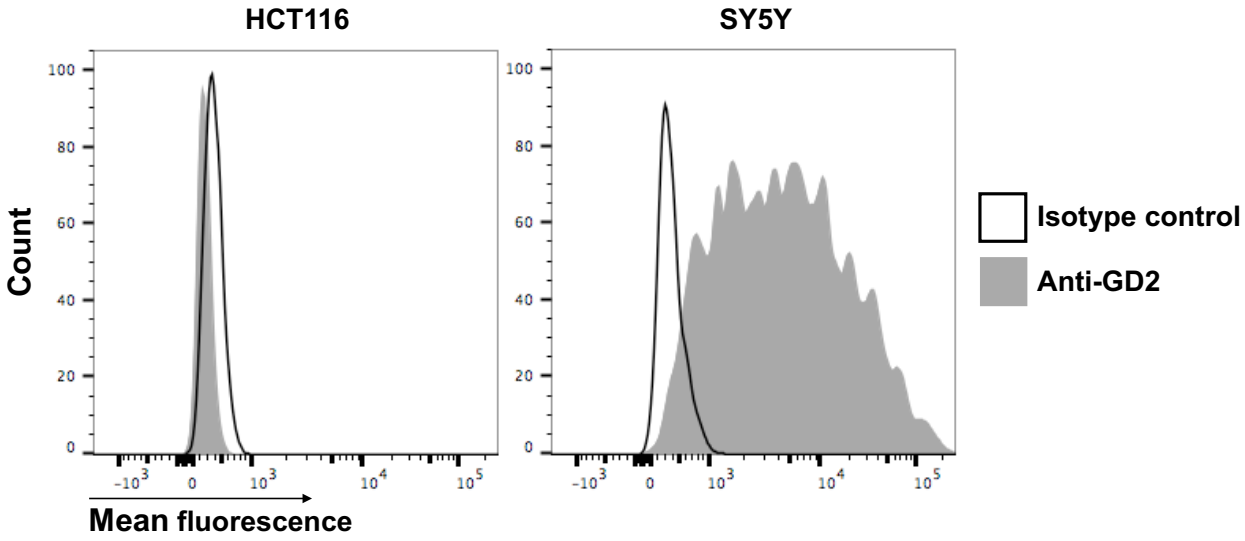

Figure S4. Analysis of GD2 expression on HCT116 and SY5Y cells with flow cytometry. HCT116 (left panel) and known GD2^{+} positive SY5Y cells (right panel) were stained with APC isotype control or APC-anti-GD2 and analyzed by flow cytometry.

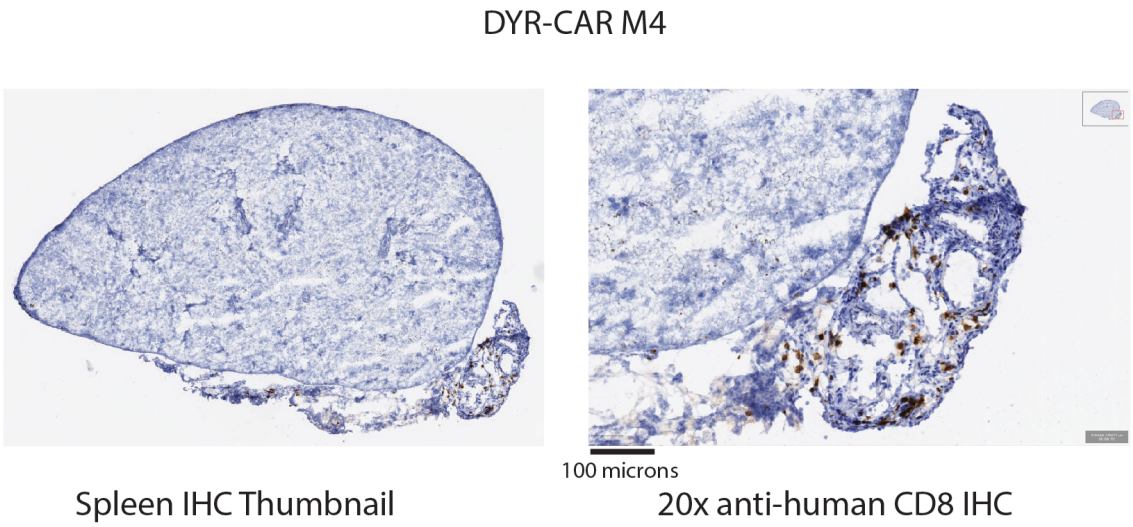

Figure S5. DYR-CAR M4 spleen. IHC was performed on the DYR-CAR M4 spleen for CD8 (see Figure 4 showing persistent PET signal from the M4 spleen on day 13). CD8 positive CAR T cells are present in the splenic periphery (20x).

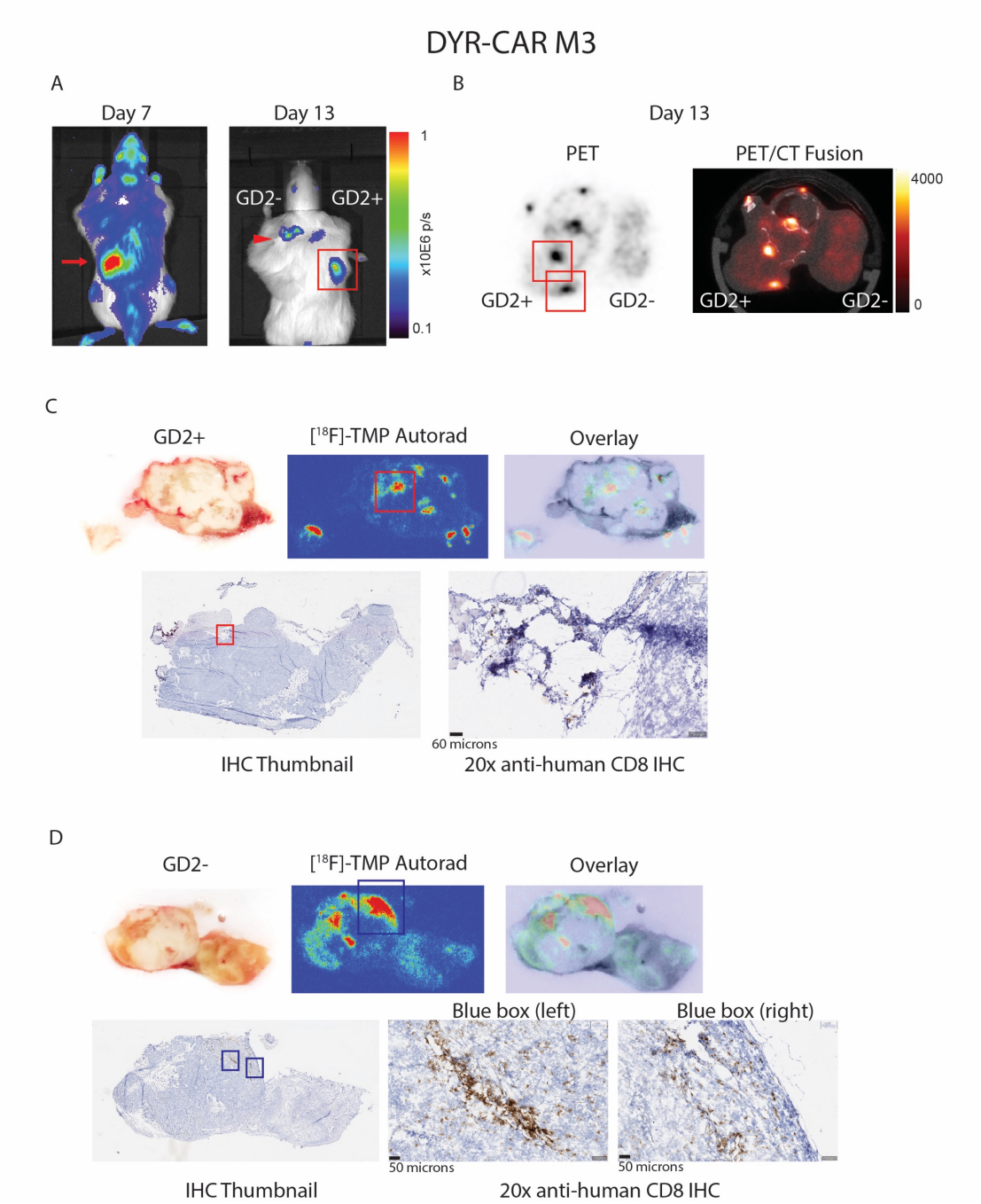

Figure S6 BLI, PET/CT, autoradiography and IHC of DYR-CAR M3 tumors. **A)** BLI shows splenic signal on D7 that decreased by D13 (arrow). New foci appear on D13 in the tumors. The areas in the GD2$^+$ 143b tumor are highlighted by the red box while the areas in the GD2$^-$ HCT116 tumor are indicated with the arrowhead. **B)** PET/CT shows foci of uptake (red boxes) in the peripheral and medial areas of the GD2$^+$ tumor and low level of generalized uptake in the GD2- tumor. **C)** Autoradiography of a section of the GD2$^+$ 143b tumor shows scattered areas of uptake and one area of radiosignal that correlates with CD8 IHC (red boxes). **D)** Autoradiography of a section of the GD2$^-$ tumor shows an area of peripheral uptake that correlates with CD8 IHC (large blue box). The small blue boxes are 20x zoom of the areas on the thumbnail image.

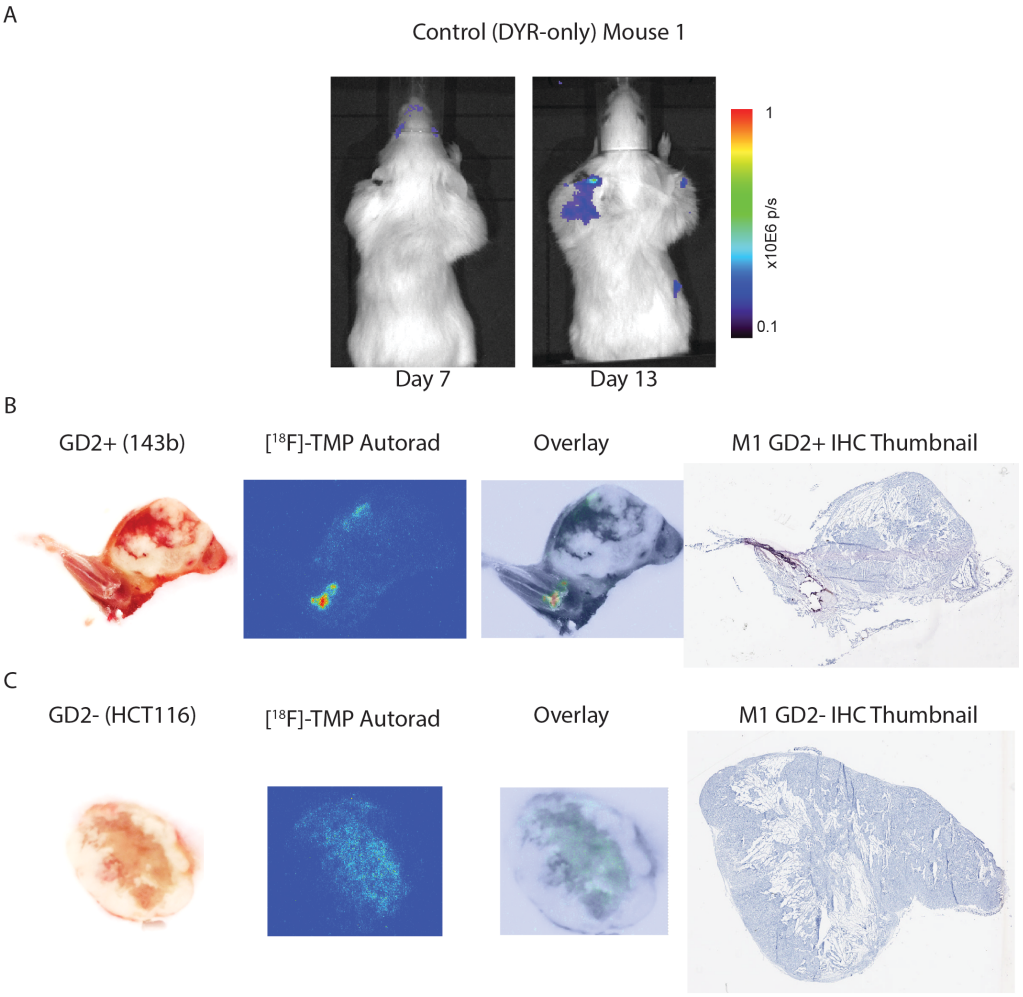

Figure S7. BLI, autoradiography and IHC of Control M1 tumors. **A)** BLI shows foci of signal overlying the HCT116 tumor ($GD2^-$). **B)** Autoradiography of the 143b tumor shows scattered areas of uptake overlying the bone of the upper arm. There were no CD8 positive T cells on IHC. **C)** The HCT116 tumor did not show any specific signal on auto-radiography and there were no CD8 positive T cells on IHC.

HLA peptide motif search results

HSV-tk

```
1      MASHAGQQHA PAFGQAARAS GPTDGRAASR PSHRQGASEA RGDPELPTLL
51     RVYIDGPHGV GKTTTSAQLM EALGPRDNIV YVPEPMTYWQ VLGASETLTN
101    IYNTQHRLDR GEISAGEAAV VMTSAQITMS TPYAATDAVL APHIGGEAVG
151    PQAPPPALTL VFDRHPIASL LCYPAARYLM GNMTPQAVLA FVALMPPTAP
201    GTNLVLGVLP EAEHADRLAR RQRPGARLDL AMLSAIRRVY DLLANTVRYL
251    QRGGRWREDW GRLTGVAAAT PRPDPEDGAG SLPRIEDTLF ALFRVPELLA
301    PNGDLYHIFA WVLDVLADRL LPMHLFVLDY DQSPVGCRDA LLRLTAGMIP
351    TRVTTAGSIA EIRDLARTFA REVGGV
```

User Parameters and Scoring Information	
method selected to limit number of results	explicit number
number of results requested	20
HLA molecule type selected	A1
length selected for subsequences to be scored	9
echoing mode selected for input sequence	Y
echoing format	numbered lines
length of user's input peptide sequence	376
number of subsequence scores calculated	368
number of top-scoring subsequences reported back in scoring output table	20

Scoring Results			
Rank	**Start Position**	**Subsequence Residue Listing**	**Score (Estimate of Half Time of Disassociation of a Molecule Containing This Subsequence)**
1	94	ASETLTNIY	67.500
2	359	IAEIRDLAR	45.000
3	43	DPELPTLLR	11.250
4	298	LLAPNGDLY	5.000
5	209	LPEAEHADR	4.500
6	82	VPEPMTYWQ	4.500
7	284	RIEDTLFAL	4.500
8	227	RLDLAMLSA	2.500
9	22	PTDGRAASR	2.500
10	41	RGDPELPTL	2.500
11	135	ATDAVLAPH	2.500
12	80	VYVPEPMTY	1.250

13	272	RPDPEDGAG	1.250
14	183	MTPQAVLAF	1.250
15	170	LLCYPAARY	1.000
16	241	DLLANTVRY	1.000
17	211	EAEHADRLA	0.900
18	165	HPIASLLCY	0.625
19	302	NGDLYHIFA	0.625
20	53	YIDGPHGVG	0.500

eDHFR

```
1      MISLIAALAV DRVIGMENAM PWNLPADLAW FKRNTLNKPV IMGRHTWESI
51     GRPLPGRKNI ILSSQPGTDD RVTWVKSVDE AIAACGDVPE IMVIGGGRVY
101    EQFLPKAQKL YLTHIDAEVE GDTHFPDYEP DDWESVFSEF HDADAQNSHS
151    YCFEILERR
```

User Parameters and Scoring Information	
method selected to limit number of results	explicit number
number of results requested	20
HLA molecule type selected	A1
length selected for subsequences to be scored	9
echoing mode selected for input sequence	Y
echoing format	numbered lines
length of user's input peptide sequence	159
number of subsequence scores calculated	151
number of top-scoring subsequences reported back in scoring output table	20

Scoring Results			
Rank	**Start Position**	**Subsequence Residue Listing**	**Score (Estimate of Half Time of Disassociation of a Molecule Containing This Subsequence)**
1	120	EGDTHFPDY	12.500
2	137	FSEFHDADA	2.700
3	25	PADLAWFKR	2.500
4	63	SSQPGTDDR	1.500
5	129	EPDDWESVF	1.250
6	67	GTDDRVTWV	1.250

7	88	VPEIMVIGG	1.125
8	77	SVDEAIAAC	1.000
9	98	RVYEQFLPK	1.000
10	116	DAEVEGDTH	0.900
11	15	GMENAMPWN	0.900
12	85	CGDVPEIMV	0.625
13	142	DADAQNSHS	0.500
14	92	MVIGGGRVY	0.500
15	18	NAMPWNLPA	0.500
16	132	DWESVFSEF	0.450
17	127	DYEPDDWES	0.450
18	4	LIAALAVDR	0.200
19	23	NLPADLAWF	0.200
20	36	LNKPVIMGR	0.125

Figure S8. Predicted half-time of dissociation to HLA class one molecules.

Ref: Parker, K. C., M. A. Bednarek, and J. E. Coligan. 1994. Scheme for ranking potential HLA-A2 binding peptides based on independent binding of individual peptide side-chains. J. Immunol. 152:163.

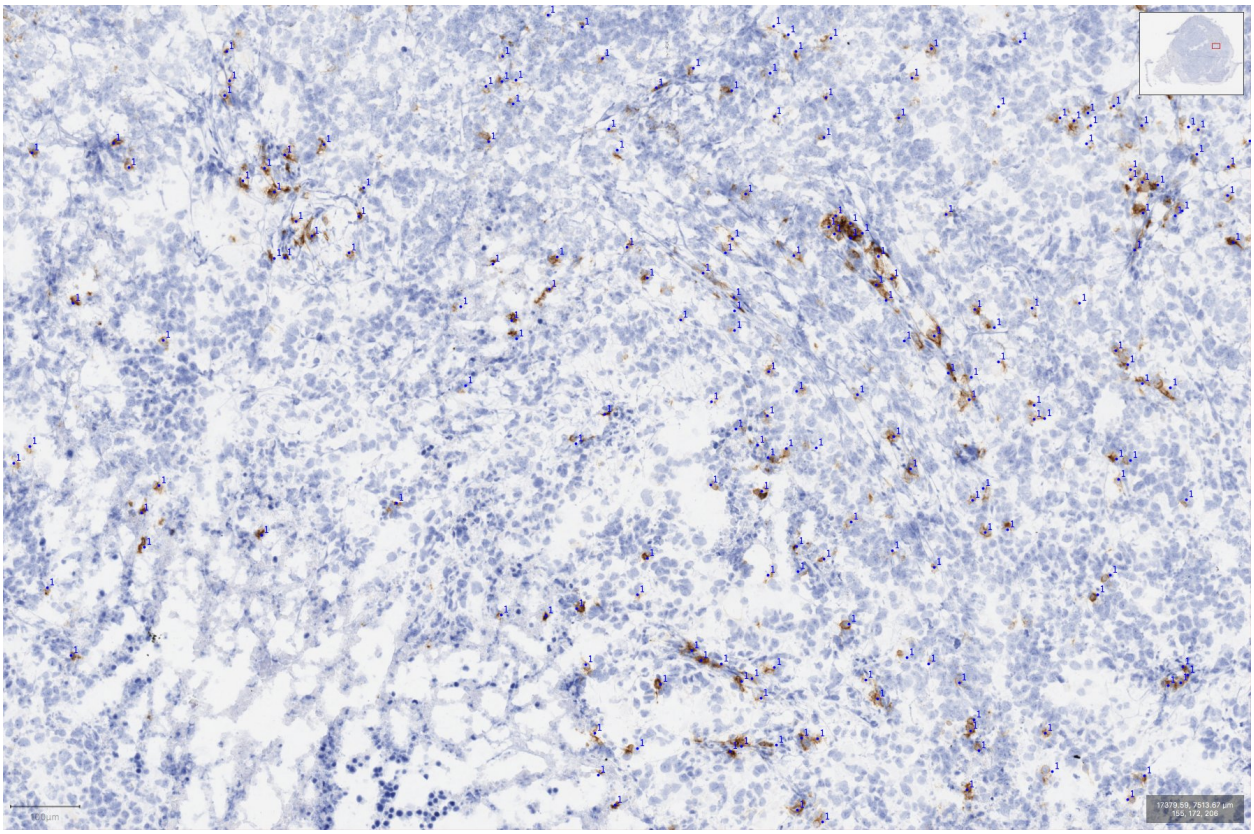

------- (100 μm)

Figure S9. Estimation of cellular density where PET signal can be determined. CD8 DYR-CAR T-cells were counted on a medium power field (10x). There are 200 cells counted (Software: Image J).

The result for calculating the volume in cu millimeters (mm^3) of a rectangular box shape, with a length of 1.65 millimeters (mm), a width (thickness) of 10 micrometers (μm) and a height of 1.1 millimeters (mm) is 0.01815 mm^3. Thus per mm^3 the number of cells needed for micro PET/CT detection is approximately (1/0.01815)*200 = (55.1)*200 = 11,000 cells per mm^3.

DYR Gene Sequence:

Ggatcc(BamHI)ATGATAAGTTTGATTGCTGCTCTGGCTGTGGACCGGGTAATCGGTATGGAA
AACGCCATGCCCTGGAACCTGCCTGCCGATTTGGCTTGGTTCAAGCGCAATACCCTGAAC
AAACCAGTAATCATGGGAAGGCATACATGGGAAAGCATTGGAAGACCACTTCCCGGTAGA
AAGAATATTATCCTGTCTAGCCAGCCCGGCACGGATGATAGGGTGACATGGGTAAAGAGC
GTCGATGAGGCGATTGCGGCGTGTGGTGACGTGCCGGAAATTATGGTTATCGGAGGCGG
CAGGGTCTACGAACAGTTCCTGCCGAAGGCACAGAAGCTGTACCTCACCCACATCGATGC
AGAGGTGGAAGGAGACACGCACTTTCCAGATTACGAGCCTGATGACTGGGAGAGTGTTTT
TAGCGAATTCCATGACGCAGACGCCCAAAACTCTCACTCCTACTGCTTTGAGATTCTCGAA
CGAAGGgcatgcgtgagcaagggcgaggagctgttcaccggggtggtgcccatcctggtcgagctggacggcgacgtaaacg
gccacaagttcagcgtgtccggcgagggcgagggcgatgccacctacggcaagctgaccctgaagttcatctgcaccaccggcaa
gctgcccgtgccctggcccaccctcgtgaccaccttcggctacggcctgcagtgcttcgcccgctaccccgaccacatgaagcagca
cgacttcttcaagtccgccatgcccgaaggctacgtccaggagcgcaccatcttcttcaaggacgacggcaactacaagacccgcg
ccgaggtgaagttcgagggcgacaccctggtgaaccgcatcgagctgaagggcatcgacttcaaggaggacggcaacatcctgg
ggcacaagctggagtacaactacaacagccacaacgtctatatcatggccgacaagcagaagaacggcatcaaggtgaacttca
agatccgccacaacatcgaggacggcagcgtgcagctcgccgaccactaccagcagaacaccccccatcggcgacggccccgtg
ctgctgcccgacaaccactacctgagctaccagtccgccctgagcaaagaccccaacgagaagcgcgatcacatggtcctgctgg
agttcgtgaccgccgccgggatcactctcggcatggacgagctgtacaagGGCAGCGGAGAGGGCAGAGGAAGT
CTTCTAACATGCGGTGACGTGGAGGAGAATCCCGGCCCTgctagcacttcgaaagtttatgatccagaac
aaaggaaacggatgataactggtccgcagtggtgggccagatgtaaacaaatgaatgttcttgattcatttattaattattatgattcaga
aaaacatgcagaaaatgctgttatttttttacatggtaacgcggcctcttcttatttatggcgacatgttgtgccacatattgagccagtagc
gcggtgtattataccagaccttattggtatgggcaaatcaggcaaatctggtaatggttcttataggttacttgatcattacaaatatcttact
gcatggtttgaacttcttaatttaccaaagaagatcatttttgtcggccatgattggggtgcttgtttggcatttcattatagctatgagcatcaa
gataagatcaaagcaatagttcacgctgaaagtgtagtagatgtgattgaatcatgggatgaatggcctgatattgaagaagatattgc
gttgatcaaatctgaagaaggagaaaaaatggttttggagaataacttcttcgtggaaaccatgttgccatcaaaaatcatgagaaagt
tagaaccagaagaatttgcagcatatcttgaaccattcaaagagaaaggtgaagttcgtcgtccaacattatcatggcctcgtgaaatc
ccgttagtaaaaggtggtaaacctgacgttgtacaaattgttaggaattataatgcttatctacgtgcaagtgatgatttaccaaaaatgttt
attgaatcggacccaggattcttttccaatgctattgttgaaggtgccaagaagtttcctaatactgaatttgtcaaagtaaaaggtcttcatt
tttcgcaagaagatgcacctgatgaaatgggaaaatatatcaaatcgttcgttgagcgagttctcaaaaatgaacaataaGTCGAC
(SalI)

DYR Protein Sequence:

MISLIAALAVDRVIGMENAMPWNLPADLAWFKRNTLNKPVIMGRHTWESIGRPLPGRKNIILSSQ
PGTDDRVTWVKSVDEAIAACGDVPEIMVIGGGRVYEQFLPKAQKLYLTHIDAEVEGDTHFPDYE
PDDWESVFSEFHDADAQNSHSYCFEILERRACVSKGEELFTGVVPILVELDGDVNGHKFSVSG
EGEGDATYGKLTLKFICTTGKLPVPWPTLVTTFGYGLQCFARYPDHMKQHDFFKSAMPEGYV
QERTIFFKDDGNYKTRAEVKFEGDTLVNRIELKGIDFKEDGNILGHKLEYNYNSHNVYIMADKQK
NGIKVNFKIRHNIEDGSVQLADHYQQNTPIGDGPVLLPDNHYLSYQSALSKDPNEKRDHMVLLE
FVTAAGITLGMDELYKGSGEGRGSLLTCGDVEENPGPASTSKVYDPEQRKRMITGPQWWARC
KQMNVLDSFINYYDSEKHAENAVIFLHGNAASSYLWRHVVPHIEPVARCIIPDLIGMGKSGKSG
NGSYRLLDHYKYLTAWFELLNLPKKIIFVGHDWGACLAFHYSYEHQDKIKAIVHAESVVDVIESW
DEWPDIEEDIALIKSEEGEKMVLENNFFVETMLPSKIMRKLEPEEFAAYLEPFKEKGEVRRPTLS
WPREIPLVKGGKPDVVQIVRNYNAYLRASDDLPKMFIESDPGFFSNAIVEGAKKFPNTEFVKVK
GLHFSQEDAPDEMGKYIKSFVERVLKNEQ